Crystallization dynamics and magnetoresistance of perovskite-like manganate synthesized by mechanical alloying

2000 J. Phys.: Condens. Matter 12 3497

(http://iopscience.iop.org/0953-8984/12/14/323)

J. Phys.: Condens. Matter **12** (2000) 3497–3503. Printed in the UK PII: S0953-8984(00)08489-7

Crystallization dynamics and magnetoresistance of perovskite-like manganate synthesized by mechanical alloying

Z Q Jin†, H X Qin, J R Zhang and Y W Du

National Laboratory of Solid State Microstructures and Institute of Solid State Physics, Department of Physics, Nanjing University, Nanjing 210093, People's Republic of China

E-mail: zqjin@nju.edu.cn

Received 7 October 1999, in final form 6 January 2000

Abstract. Nanocrystalline ferromagnetic $La_{0.7}Ca_{0.3}MnO_3$ perovskites with magnetoresistance effect have been successfully prepared by mechanical alloying. Thermal transformation of the amorphous phase, resulting from ball milling, to perovskite structure was studied by differential scanning calorimetry. Following the law of mass action, we discuss the crystallization dynamics of the amorphous phase. The activation energy for crystallization transformation is calculated to be about +1.25 kJ g^{-1}. The characterization of resistivity $\rho(T)$ for $La_{0.7}Ca_{0.3}MnO_3$ perovskites has also been investigated. At low temperature T, $\rho(T)$ has a direct-proportion dependence on T^2. With increasing annealing temperature, the slope of the ρ–T^2 curve decreases. The temperature dependent magnetoresistance effect at temperature far below the Curie temperature can be well expressed as the equation $\Delta\rho/\rho_0 = p_1 - p_2T^{3/2} - p_3T^{5/2}$.

1. Introduction

In recent years, the rare-earth manganate perovskites, of which the prototype is $Ln_{1-x}A_xMnO_3$ (Ln = La, Pr, Nd, Sm; A = Ca, Sr, Ba, Pb) have attracted considerable attention in scientific studies and potential technological application due to their giant magnetoresistance effect [1–4]. This effect has been investigated in polycrystalline pellets [5] single crystals [6] and thin films [7]. Most of the investigations show that the ferromagnetic Curie temperature, the low-temperature magnetoresistance and the metal–semiconductor transition in such materials are strongly dependent on the preparation routine and are markedly affected by grain size. Ultrafine manganese oxides powders were usually prepared via a citrate–gel route or by a standard ceramics method [4, 8, 9]. However, their applications are limited due to low yield rates and complexity of preparation procedures. For instance, by using the citrate–gel technique, one needs the following complex preparation procedure: dissolution, low-temperature evaporation, thermal treatment, grinding and final calcination usually above 1473 K to synthesize the compound. The calcining temperature necessary in the crystallization process is a little higher and the size of particles produced is beyond the nanometre. Therefore, the challenge of improving the preparation method still remains. Mechanical alloying has been reported to be one of the simplest techniques to prepare magnetic alloys [10] and ferrite powders [11], and presents unique advantages including its low-temperature synthesis (around 1073 K) and high yield rate for preparation of fine homogeneous particles. In this work, the ultrafine polycrystalline ferromagnetic $La_{0.7}Ca_{0.3}MnO_3$ perovskite has been fabricated by mechanical

† Corresponding author: Zhi-qiang Jin.

0953-8984/00/143497+07$30.00

alloying and subsequent heat treatment, which may be useful for further investigation of new MR materials. In addition, as well known, milling for a certain period of time may result in the occurrence of an amorphous phase which usually transforms into a crystal structure during subsequent heat treatment. Consequently, we carried out a systematic dynamical-behaviour study on the transformation in order to understand the effects of processing temperature. The activation energy for this transformation has been calculated through the law of mass action. Meanwhile, we have also investigated the dependences of resistivity and magnetoresistance on temperature experimentally.

2. Experimental procedure

La hydroxide and Ca and Mn carbonate powders were used in this study. Appropriate amounts of the hydroxide and carbonates with molar ratios of La/Ca/Mn of 0.7/0.3/1 were ground in a hardened steel vial together with 11 mm steel balls for 10–100 h using a centrifugal planetary ball mill. The contamination of α-Fe from the mill is not significant in this case and can be neglected after magnetic separation. The milled powders were then pressed into discs. Annealing the discs was carried out at 823–1473 K for 1 h. All powder handling, milling and subsequent pressing and heat treatment were performed in air. The densities of disc samples after annealing were in the range of 4–4.5 g cm^{-3}.

The resulting powders were identified by x-ray diffraction (XRD) analysis using a Rigaku D/Max-γA diffractometer with Cu Kα radiation. This technique allowed us to monitor structural change and the degree of alloying. Particle dimension and morphology of the powders were observed using scanning electron microscopy. After milling for 100 h, the sample presented an amorphous structure. Differential scanning calorimetry (DSC) measurement with a heating rate of 2.0 K min^{-1} was used to detect the crystallization temperature of the amorphous sample and to analyse its dynamical behaviour. The electrical resistivity of the discal sample was measured as a function of temperature and magnetic field using the conventional dc four-probe technique. Data were collected between 77 K and 300 K in magnetic fields up to 1.5 T. In the measurements of MR, the applied field was perpendicular to a constant current. The MR ratio was usually defined as $\Delta\rho/\rho_0 = [\rho(T, 0) - \rho(T, H)]/\rho(T, 0)$, where $\rho(T, H)$ and $\rho(T, 0)$ were the resistivity in an applied magnetic field and zero-field resistivity, respectively.

3. Results and discussion

During the milling process, powders are heavily deformed and cold-welded by colliding balls, leading to the formation of characteristically layered particles with a large amount of strain. Further milling leads to a refinement of the layered microstructure. Scanning electron micrographs of samples milled for 100 h show that the layered particles have a size distribution in the range of 0.2–2 μm. XRD profiles of powders after milling for different times and annealing at various temperatures are taken. The representative XRD patterns (figure 1) indicate that after milling for 100 h, the intensity of the XRD characteristic of precursor compounds almost disappears completely; meanwhile, an amorphous characteristic pattern builds up. It should be pointed out that perovskite phase cannot be obtained when the samples are annealed for 1 h below 823 K. The subsequent heat treatment at low temperature only results in the relief of most of the strain. However, after annealing at 873 K, some new diffraction peaks are detected in addition to the amorphous characteristic pattern, indicating the formation of crystallites. Above 973 K the samples crystallize completely into a single phase. All the

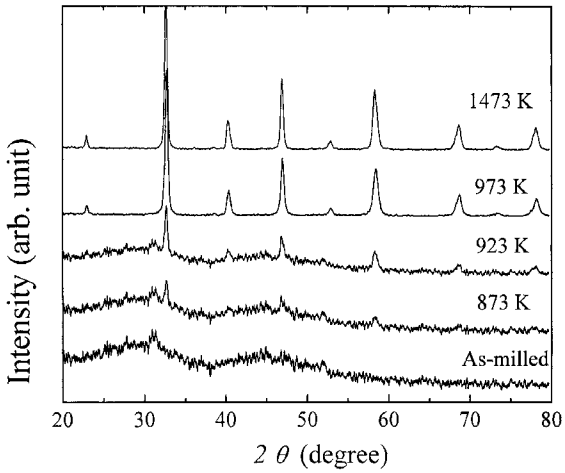

Figure 1. X-ray diffraction patterns of mechanically alloyed $La_{0.7}Ca_{0.3}MnO_3$ samples after milling for 100 h, and subsequent annealing at different temperatures.

patterns index well on the characteristic peaks of the perovskite $La_{0.7}Ca_{0.3}MnO_3$ structure. No traces of other phases are detectable. The lattice parameter a of perovskite powders is calculated from the XRD pattern to be in the range of 7.726–7.733 Å, which is close to the literature value of 7.719–7.731 Å [4]. Analysis of the line-width of the diffraction pattern of the annealed samples, using the Scherrer formula, provides an average grain size [12]. The results show that the grain size in the samples annealed at 973 K is around 30 nm, and the grains grow rapidly to 300 nm with increasing annealing temperature up to 1473 K.

In the inset of figure 2, the DSC spectrum for an amorphous sample is shown. The main panel of figure 2 gives its locally amplified pattern after the background has been subtracted. An obvious exothermic peak can be found in the range of 863–963 K, which should be attributed to the crystallization of the amorphous phase as determined in figure 1. The temperature of 920 K, at which the maximum in the peak occurs, might be assumed to be the crystallization temperature. Moreover, the exothermic heat H_t of 53 J g^{-1} is also obtained. Here, H_t has the meaning of $H_t = \int_{T_0}^{\infty} \mathrm{d}H_p/\mathrm{d}t$, where t is processing time during the DSC measurement and H_p and H_t denote the exothermic heats of partial and complete crystallization, respectively. $H_q = H_t - H_p$ has been given as a shaded area in figure 2. Moreover, the fraction of crystalline precipitate $La_{0.7}Ca_{0.3}MnO_3$ in the amorphous matrix after processing at temperature T_p is characterized by $F = H_p/H_t$. The fraction F as a function of T_p (as given in figure 2) clearly shows that no crystallites precipitate from the amorphous matrix below 863 K. However, above 863 K, a small amount of crystallites begin to precipitate out. It can be seen that the fraction of crystallites increases with increasing T_p, and reaches a value of 50% at 920 K. For samples annealed at temperature higher than 920 K, H_p/H_t rises rapidly to a value of 100%, indicating a complete crystallization of the amorphous phase. This is in good agreement with x-ray data.

The dynamical behaviour of the crystallization of the amorphous phase is discussed as follows by referring to the DTA results. As is well known, the amorphous phase with higher free energy than that of the equilibrium state is always in a metastable state and would transform into a crystallite under certain kinds of condition. The activation energy for this transformation can be defined as E. If we assume that $\mathrm{d}F/\mathrm{d}t$ represents the crystallization velocity, then following the law of mass action, the dynamical behaviour may be written in standard notation

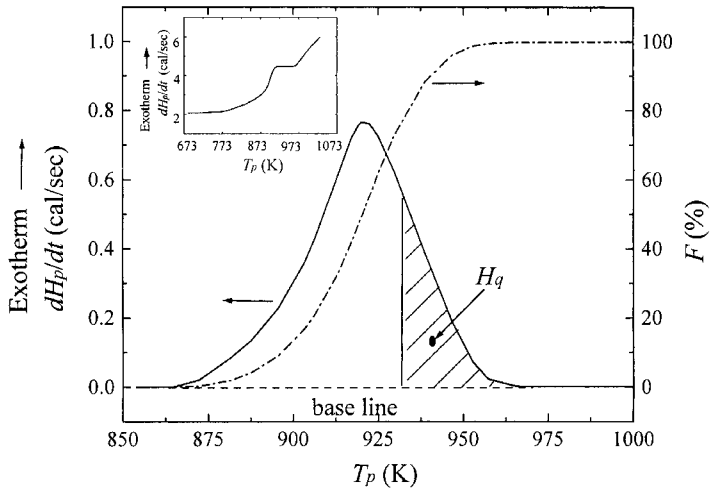

Figure 2. DTA spectra (inset), and its locally amplified pattern with background subtracted, and the crystallization fraction F dependence of processing temperature T_p for a milled $La_{0.7}Ca_{0.3}MnO_3$ sample. H_q is defined as $H_q = H_t H_p$, where H_p and H_t denote the exothermic heats of partial and complete crystallization, respectively.

as:

$$\mathrm{d}F/\mathrm{d}t = k(1-F)^n. \tag{1}$$

Here n is the reaction series; k has an Arrhenius dependence on temperature T_p,

$$k = A\exp(-E/RT_p) \tag{2}$$

where A is a coefficient, R is the gas constant. Since H_t is a constant for a certain reaction, then by inserting $F = H_p/H_t$ into equation (1), we have

$$H_t^{-1}(\mathrm{d}H_p/\mathrm{d}t) = A(1-H_p/H_t)^n\exp(-E/RT_p). \tag{3}$$

By considering $H_q = H_t - H_p$ and through logarithmic computation, the above formula can be rewritten as

$$\ln(\mathrm{d}H_p/\mathrm{d}t) - \ln H_t = \ln A + n\ln H_q - n\ln H_t - (E/R)T_p^{-1}. \tag{4}$$

According to the difference approach, we can obtain a new expression

$$\Delta\ln(\mathrm{d}H_p/\mathrm{d}t) = -(E/R)\Delta T_p^{-1} + n\Delta\ln H_q. \tag{5}$$

Figure 3 presents the dependence of $\Delta\ln(\mathrm{d}H_p/\mathrm{d}t)/\Delta\ln H_q$ on $\Delta T_p^{-1}/\Delta\ln H_q$. It can be found that the calculated results (scatter points) can be fitted quite well with a line using equation (5). From the line slope $-E/R$, the activation energy E of the transformation from the amorphous phase into crystallites can be well estimated to be about 1.25 kJ g^{-1} which is larger than the activation energy of chemical diffusion of about 0.36 kJ g^{-1} for $La_{0.7}Sr_{0.3}CoO_{3-\delta}$ [14]. This may be attributed to the existence of a large amount of stress in the as-milled sample.

In this investigation, all the samples annealed above 973 K exhibit magnetoresistance characteristics. The temperature T as a function of both resistivity ρ and magnetoresistance ratio $\Delta\rho/\rho_0$ with applied external fields $H = 0$ and 1.5 T for the representative sample annealed at 1273 K is shown in figure 4. There is a peak in the ρ–T curve, indicating a metallic character ($\mathrm{d}\rho/\mathrm{d}T > 0$), below and an insulating character ($\mathrm{d}\rho/\mathrm{d}T < 0$) above this temperature. It can be seen that the metal–insulator transition is smooth but not sharp, which is similar to the

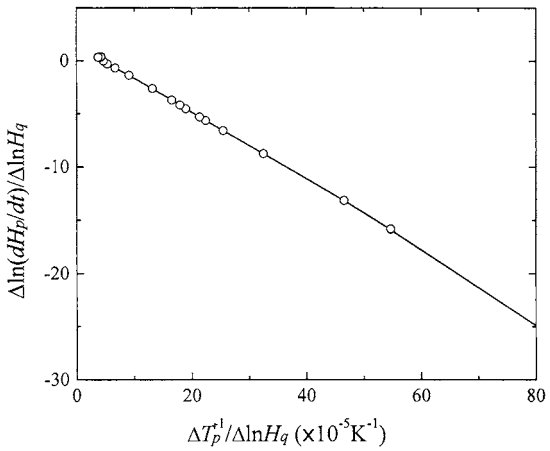

Figure 3. $\Delta \ln(\mathrm{d}H_p/\mathrm{d}t)/\Delta \ln H_q$ dependence of $\Delta T_p^{-1}/\Delta \ln H_q$. The definitions of these parameters have been given in the text.

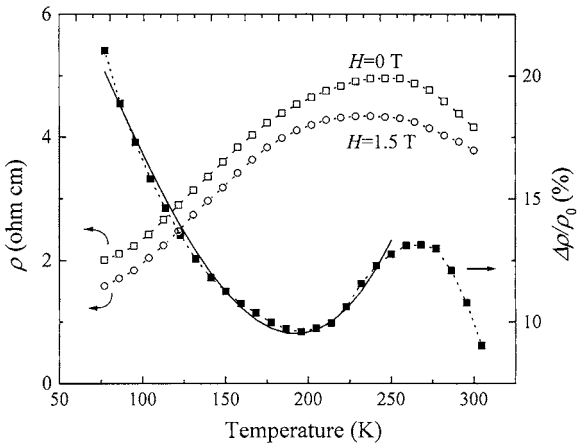

Figure 4. Temperature variation of resistivity and magnetoresistance at $H = 0$ and 1.5 T for $La_{0.7}Ca_{0.3}MnO_3$ samples annealed at 1273 K. The low-temperature magnetoresistance effect below 200 K can be well fitted to the function of $p_1 - p_2T^{3/2} - p_3T^{5/2}$ (solid curve).

results observed in nanocrystalline $La_{0.7}Ca_{0.3}MnO_3$ perovskite [4]. Moreover, figure 4 also shows that the expression $\Delta\rho/\rho_0 = p_1 - p_2T^{3/2} - p_3T^{5/2}$ can nicely describe the temperature dependence of the MR effect quite well for $T < 200$ K. Experimentally, Fontcuberta *et al* [13] have demonstrated that the resistivity follows a law of $\rho(T, H)/\rho(T, 0) = 1 - Bm^2(T)$, where the B parameter reflects an intrinsic characteristic of the sample, $m = M(H, T)/M_s$ is a reduced magnetization which can be described under a certain applied field by the Dyson equation

$$m = 1 - a_0(T/T_C)^{3/2} - a_1(T/T_C)^{5/2} - a_2(T/T_C)^{7/2} - a_3(T/T_C)^4 \qquad (6)$$

where T_C is Curie temperature. Therefore, by considering $\Delta\rho/\rho_0 = [\rho(T, 0) - \rho(T, H)]/\rho(T, 0)$, and putting m into $Bm^2(T)$, one obtains

$$\Delta\rho/\rho_0 = B[(1 - 2a_0(T/T_C)^{3/2} - 2a_1(T/T_C)^{5/2} - \cdots]. \qquad (7)$$

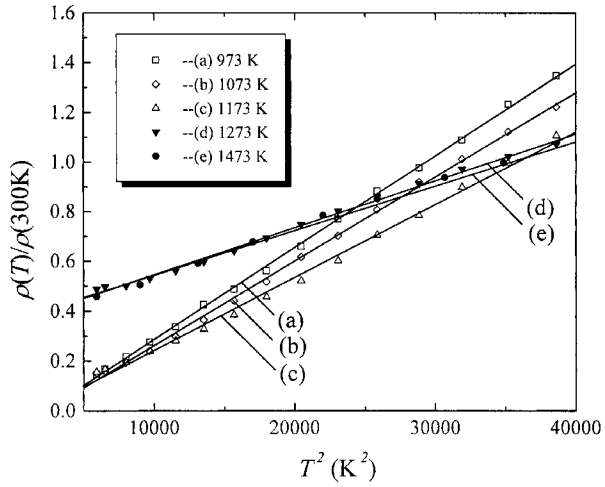

Figure 5. The relation between the temperature T and normalized resistivity $\rho(T)/\rho(300\ \mathrm{K})$ at zero field. The experimental data can be well fitted to the $\rho(T)/\rho(300\ \mathrm{K}) = b_1 + b_2T^2$ expression.

Our fitting function $\Delta\rho/\rho_0 = p_1 - p_2T^{3/2} - p_3T^{5/2}$, when replacing p_1 with B, p_2 with $2a_0B/T_C^{3/2}$ and p_3 with $2a_1B/T_C^{5/2}$, respectively, is in good agreement with the first two terms of equation (7). Therefore, the function may be reasonable to interpret the low-temperature MR effect. However, it is noteworthy that the fitted parameter ($p_1 = 0.30$) in the present work is smaller than the result ($B = 0.66$) taken from [13]. The discrepancy may be attributed to the fact that the simplified model is applied in the present investigation and the range of temperatures may not be sufficient for quantitative estimations. Figure 5 depicts the relation between T^2 and $\rho(T)/\rho(300\ \mathrm{K})$. In the range of temperature far below the peak temperature, the relationship of $\rho(T)/\rho(300\ \mathrm{K})$ with T^2 can be expressed as $\rho(T)/\rho(300\ \mathrm{K}) = b_1 + b_2T^2$ (i.e. $\mathrm{d}\rho(T)/\mathrm{d}T \sim T$). The temperature-dependent resistivity is generally considered to be related to d electron scattering (spin-disorder scattering) and spin-wave scattering [11]. Moreover, it can be seen that the coefficient b_2 decreases with increasing annealing temperature which may be attributed to the grain growth [12].

4. Conclusions

Mechanical alloying has been applied to fabricate single-phase $La_{0.7}Ca_{0.3}MnO_3$ compounds with giant magnetoresistance effect. It is found that after milling for 100 h, particle samples exhibit an amorphous structure. After annealing above the crystallization temperature, perovskite-type crystallites are present in the samples. The crystallization process and dynamical behaviour on the formation of the crystallites have been investigated according to the law of mass action. The apparent activation energy for the amorphous–crystalline phase transition has been calculated to be about 1.25 kJ g^{-1}. All the samples annealed above 973 K exhibit an apparent low-temperature MR effect. The dependences of resistivity $\rho(T)$ and MR ratio $\Delta\rho/\rho_0$ on temperature T can be described with expressions of $\rho(T)/\rho(300\ \mathrm{K}) = b_1 + b_2T^2$ and $\Delta\rho/\rho_0 = p_1 - p_2T^{3/2} - p_3T^{5/2}$, respectively. They may be reasonable to interpret low-temperature resistivity behaviour.

Acknowledgments

Supported by NMS and NSFC projects, People's Republic of China.

References

[1] Barrette J, Lees M R, Balakrishnan G and Paul D McK 1996 *Appl. Phys. Lett.* **68** 424
[2] Moritomo Y, Asamitsu A and Tokura Y 1995 *Phys. Rev.* B **51** 16 491
[3] Coey J M D, Viret M, Ranno L and Ounadjela K 1995 *Phys. Rev. Lett.* **75** 3910
[4] Mahesh R, Mahendiran R, Raychaudhuri A K and Rao C N R 1995 *Appl. Phys. Lett.* **68** 2291
[5] Jin S, O'Bryan H M, Tiefel T H, McCormack M and Rhodes W W 1995 *Appl. Phys. Lett.* **66** 382
[6] Liu J Z, Chang I C, Irons S, Klavins P and Shelton R N 1995 *Appl. Phys. Lett.* **66** 3218
[7] Bae S Y and Wang S X 1996 *Appl. Phys. Lett.* **69** 121
[8] Mahendiran R, Mahesh R, Raychaudhuri A K and Rao C N R 1995 *Solid State Commun.* **94** 515
[9] Guo Z B, Zhang J R, Zhang N, Ding W P, Huang H and Du Y W 1997 *Appl. Phys. Lett.* **70** 1897
[10] Schultz L, Wecker J and Hellstern E 1987 *J. Appl. Phys.* **61** 3583
[11] Jin Z Q, Tang W, Zhang J R, Lin H and Du Y W 1998 *J. Magn. Magn. Mater.* **182** 231
[12] Jin Z Q, Zhang J R, Tang W and Du Y W 1998 *Solid State Commun.* **108** 867
[13] Fontcuberta J, Martínez B, Seffar A, Piñol S, García-Muñoz J L and Obredors X 1996 *Phys. Rev. Lett.* **76** 1122
[14] Kononchuk O F, Sutija D P, Norby T and Kofstad P 1995 *Proc. 4th Int. Symp. on Solid Oxide Fuel Cells (Yokohama)* p 395